ELSEVIER

Physica E 13 (2002) 965–968

PHYSICA E

www.elsevier.com/locate/physe

High thermoelectric figure of merit ZT in PbTe and Bi_2Te_3-based superlattices by a reduction of the thermal conductivity

H. Beyer[a,*], J. Nurnus[a], H. Böttner[a], A. Lambrecht[a], E. Wagner[a], G. Bauer[b]

[a] *Frainhofer Institut Physikalische Messtechnik, Heidenhofstr. 8, D-79110 Freiburg i. Br., Germany*
[b] *Institut für Halbleiterphysik, Johannes Kepler-Universität Linz, Altenbergerstraße 69, A-4040 Linz, Austria*

Abstract

Experimental evidence is presented for an enhanced thermoelectric figure of merit $ZT = \sigma S^2 T/\lambda$ (where σ is the electrical conductivity, S the thermopower, T the temperature, and λ is the thermal conductivity) by a reduction of the thermal conductivity λ in PbTe- and Bi_2Te_3-superlattices (SLs) parallel to the layer planes. Data on thermoelectric properties of $Bi_2Te_3/Bi_2(Se_xTe_{1-x})_3$-SLs, of PbTe-based doping SLs, and $PbTe/PbSe_{0.2}Te_{0.8}$-SLs are presented. In these structures, a decrease of λ was measured compared to the corresponding bulk compounds or homogeneous alloys. Despite a drop of the total power factor σS^2 in the SLs in total an enhancement of the figure of merit ZT is found in these highly-doped PbTe and Bi_2Te_3-based SLs. © 2002 Elsevier Science B.V. All rights reserved.

Keywords: Thermoelectrics; Superlattices; Thermal conductivity; Figure of merit

In low-dimensional structures, an enhancement of the thermoelectric figure of merit $ZT = \sigma S^2 T/\lambda$ (where σ is the electrical conductivity, S the thermopower, and λ is the thermal conductivity) is predicted (for a recent review see Ref. [1]). As calculated and experimentally verified in Refs. [2,3], a ZT-rise for transport parallel to the layer plane due to carrier quantum confinement is only possible in the confinement layers. ZT-rises of the whole structure can be achieved by a reduction of the thermal conductivity λ either due to phonon confinement and/or enhanced phonon scattering mechanisms. A reduction of the thermal conductivity in Bi_2Te_3-based superlattices was predicted for transport both perpendicular [4] and parallel [5,6] to the SL layer planes. Experimental evidence for a reduced thermal conductivity parallel to the layer plane was previously reported for GaAs/AlAs-SLs [7] and Si/Ge-SLs [8,9]. Calculations [10] and experiments [11] show that the incorporation of ultra-narrow layers of dissimilar materials like C into Si results in a significant λ-reduction. Furthermore, rather large ZT-values were observed for PbTe/Te- [12] and $PbTe/PbSe_{0.98}Te_{0.02}$-quantum dot superlattices [13]. In the latter case, a record ZT value of 0.75 at room temperature and of 2.0 at $T = 560$ K was reported and attributed also to a reduction of λ.

In the present study, the figure of merit ZT in MBE-grown superlattices based on PbTe and Bi_2Te_3 is investigated for transport parallel to the layer planes. In the V–VI-material system symmetric $Bi_2(Se_xTe_{1-x})_3/Bi_2(Se_yTe_{1-y})_3$-SLs (#Bi1–#Bi4) with different periods and Se-contents were grown.

* Corresponding author. Tel.: +49/(0)7-61/88-57-411; fax: +49/(0)7-61/88-57-224.
E-mail address: harald.beyer@ipm.fhg.de (H. Beyer).

1386-9477/02/$ - see front matter
PII: S1386-9477(02)00246-1

Table 1
Structural and experimentally determined transport parameters of the investigated Bi_2Te_3- and PbTe-based superlattice structures

#	Se-content x/y	SL periods	period (nm)	carrier conc. 10^{18} (cm^{-3})	σS^2 ($\mu W\,cm^{-1}\,K^{-2}$)
n-type symmetric $Bi_2(Se_xTe_{1-x})_3/Bi_2(Se_yTe_{1-y})_3$-superlattices					
Bi1	0/0.12	50	20	44	32
Bi2	0/0.12	100	10	40	27
Bi3	0.06/0.12	100	12	42	25
Bi4	0/0.33	225	4	26	16
n-type PbTe/$PbSe_{0.20}Te_{0.80}$-SLs, nominal $d_{PbSeTe} = 1.8$ nm					
Pb1		155	15.5	6.8	25.5
Pb2		360	6.7	6.2	27.1
Pb3		490	5.2	5.8	26.9
Pb4		660	4.2	5.9	25.9
p-type PbTe doping SLs (nominal 0.8 nm BaF_2-doped layer)					
Ba1		270	9.9	12	24.4
Ba2		460	5.7	12	25.2

Furthermore, n-type-doped PbTe/$PbSe_{0.20}Te_{0.80}$-SLs (#Pb1–Pb4) were investigated with a fixed $PbSe_{0.20}Te_{0.80}$-layer thickness of nominal $d_{PbSeTe} = 1.8$ nm. In addition, p-type PbTe-doping superlattices were investigated, where a thin layer with a high doping concentration (nominal 0.8 nm BaF_2-doped layer, $p_{BaF2} > 10^{20}$ cm^{-3}) acts as an incorporated layer of a dissimilar material. The period of the superlattices was varied by a variation of the PbTe-layer widths, keeping the width of the incorporated layers constant. The most important structural and measured thermoelectric parameters of the investigated structures are listed in Table 1.

$Bi_2(Se_xTe_{1-x})_3/Bi_2(Se_yTe_{1-y})_3$-SLs were grown by molecular beam epitaxy (MBE) on freshly cleaved $BaF_2(1\,1\,1)$ substrates at a substrate temperature of 290°C. Bi and Te element sources and an Se-valved cracker cell were used. Bi_2Te_3- and $Bi_2(Se_xTe_{1-x})_3$-films were deposited using a flux ratio of Bi/(Te + Se) = $\frac{5}{12}$. PbTe(1 1 1)-based superlattices on $BaF_2(1\,1\,1)$ were grown at a substrate temperature of 370°C. PbTe was evaporated from a PbTe-compound source, achieving a growth rate of 1.5 $\mu m\,h^{-1}$. An additional Te-flux (10%) was used to stabilize the stoichiometry. N-type doping was achieved by elementary bismuth, and p-type doping by BaF_2. $PbSe_{0.20}Te_{0.80}$-layers were grown by an additional PbSe-flux from a PbSe-compound source. The structural quality of the superlattices was investigated by X-ray diffraction and secondary ion mass spectroscopy (SIMS) [14,15]. Thermal conductivity measurements on thin films were performed by a bridge method described in Ref. [16] for electrically conducting films with a significant temperature coefficient of the electrical resistance. Heat losses due to radiation and the heat flux through the thin film are based on the balance of Joule heating due to an electric current through the unsupported epilayer.

For symmetric $Bi_2(Se_xTe_{1-x})_3/Bi_2(Se_yTe_{1-y})_3$-SLs, power factors between 28 and 35 $\mu W\,cm^{-1}\,K^{-2}$ are determined for periods above 10 nm (#Bi1–#Bi3). This is a reduction between 15% and 30% compared to epitaxial Bi_2Te_3-films and is mostly attributed to a reduction of the carrier mobility in the SLs with respect to the homogeneous Bi_2Te_3-films. A power factor of 15 $\mu W\,cm^{-1}\,K^{-2}$ is found for the $Bi_2Te_3/Bi_2(Se_{0.33}Te_{0.67})_3$-SL with 4 nm period (#Bi4). This is attributed to a lower thermopower of the crystalline phase Bi_2Te_2Se ($x = 0.33$) compared to Bi_2Te_3 and the lower carrier concentration of $n = 2.8 \times 10^{19}$ cm^{-3}. For n-type PbTe/$PbSe_{0.20}Te_{0.80}$-SLs (#Pb1–#Pb4) with nominal $n = 6 \times 10^{18}$ cm^{-3} a nearly constant power factor of about 26.5 $\mu W\,cm^{-1}\,K^{-2}$ (n-type) is found to be independent of the superlattice period. This drop in the power factor of 20–30% is related to a drop in the carrier mobility. In PbTe-doping-SLs with $p = 1.2 \times 10^{19}$ cm^{-3}, power factors between 24 and

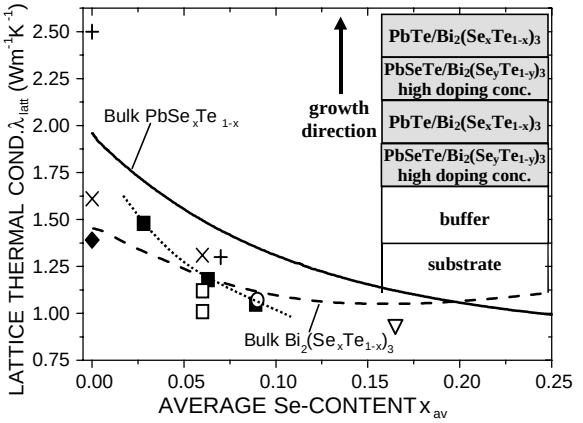

Fig. 1. Experimentally determined lattice thermal conductivity at $T = 300$ K of PbTe- and Bi_2Te_3-based superlattice structures (symmetric $Bi_2(Se_xTe_{1-x})_3/Bi_2(Se_yTe_{1-y})$-SLs: $x = 0/y = 0.12$, #Bi1, #Bi2 (□); $x = 0.06/y = 0.12$, #Bi3 (◯); $x = 0/y = 0.33$, #Bi4 (▽). N-type $PbTe/PbSe_xTe_{1-x}$-SLs, nominal $d_{PbSeTe} = 1.8$ nm, #Pb1, #Pb3, #Pb4 (the dotted line is a guide for the eye) (■); p-type doping SLs, nominal 0.8 nm BaF_2-doped layer, #Ba2 (♦)) compared to homogeneous $PbSe_xTe_{1-x}$- (+) and $Bi_2(Se_xTe_{1-x})_3$- (×) epitaxial films and literature values of bulk materials [16,17]. The inset shows a scheme of the investigated superlattice structures.

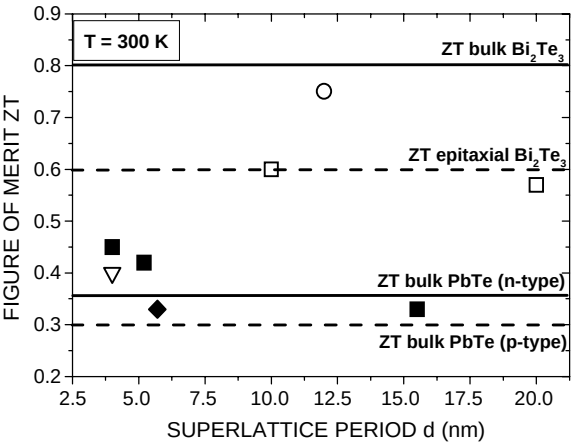

Fig. 2. Room temperature figure of merit ZT vs. SL-period of different $Bi_2(Se_xTe_{1-x})_3/Bi_2(Se_yTe_{1-y})$-SLs and PbTe-based SL structures compared to bulk materials and homogeneous epitaxial layers (V–VI-materials). Symmetric $Bi_2(Se_xTe_{1-x})_3/Bi_2(Se_yTe_{1-y})$-SLs: $x = 0/y = 0.12$, #Bi1, #Bi2 (□); $x = 0.06/y = 0.12$, #Bi3 (◯); $x = 0/y = 0.33$, #Bi4 (▽). N-type $PbTe/PbSe_xTe_{1-x}$-SLs, nominal $d_{PbSeTe} = 1.8$ nm, $n = 6 \times 10^{18}$ cm^{-3}, #Pb1, #Pb2, #Pb4 (■); p-type doping SL, $p = 1.2 \times 10^{19}$ cm^{-3}, nominal 0.8 nm BaF_2-doped layer, #Ba2 (♦).

28 μW cm^{-1} K^{-2} were determined, which is rather a small reduction compared to bulk p-PbTe (maximum 30 μW cm^{-1} K^{-2}).

The lattice thermal conductivity λ_{latt} was calculated from the measured thermal conductivity λ by $\lambda_{latt} = \lambda - \lambda_{el}$, where for the subtraction of the electronic contribution $\lambda_{el} = L\sigma T$ (where L is the Lorentz number, σ the electrical conductivity, and T is the temperature) was used. A room temperature Lorentz number of 2.2×10^{-8} W Ω K^{-2} was used for $PbTe/PbSe_{0.20}Te_{0.80}$-SLs with $n = 6 \times 10^{18}$ cm^{-3}, of 2.45×10^{-8} W Ω K^{-2} for the doping superlattice with $p = 1.2 \times 10^{19}$ cm^{-3} according to Ref. [17], and of 1.2–1.4 $\times 10^{-8}$ W Ω K^{-2} for the Bi_2Te_3-based SLs. The λ_{latt}-values determined from the measured results are compared to the data for ternary bulk $Bi_2(Se_xTe_{1-x})_3$- [18] and $PbSe_xTe_{1-x}$-alloys [19] and epitaxial ternary layers with an Se-content corresponding to the average Se-content x_{av} of the SL structures (Fig. 1). Increasing the average Se-content x_{av} decreases the lattice thermal conductivity in the SLs. A particularly strong drop of λ_{latt} to 1.4 W m^{-1} K^{-1} was found for the PbTe-doping (BaF_2) SL with 5.7 nm period (#Ba2) compared to PbTe.

The comparison between the figure of merit of Bi_2Te_3-single layers (ZT = 0.6) and Bi_2Te_3-based SLs is shown in Fig. 2. The ZT-values of the SLs (#Bi1–#Bi3) are as high as the ZT-values of the Bi_2Te_3-epitaxial layers due to the λ-reduction described above. For the SL with 4 nm period (#Bi4) containing Bi_2Te_2Se (according to $x = 0.33$), a ZT-value of 0.4 was determined. For the p-type PbTe-doping SL with 5.7 nm period and $p = 1.2 \times 10^{19}$ cm^{-3} (#Ba2) ZT = 0.33 was determined, which corresponds to a ZT-enhancement by 10% compared to the best p-type PbTe-epilayers and by about 20% compared to bulk PbTe with the same doping level. An even stronger ZT-enhancement is found for $PbTe/PbSe_{0.20}Te_{0.80}$-SLs with $n = 6 \times 10^{18}$ cm^{-3} (#Pb1, #Pb3, #Pb4) with ZT-values up to 0.45 for the structure with a period of 4.2 nm. Apparently, the reduction of the power factors is overcompensated by the reduction of the thermal conductivity and results in a ZT-enhancement by 20–25%.

The optimum ZT-values for the two material systems are found for quite different temperatures. In Fig. 3, the temperature dependence of ZT for

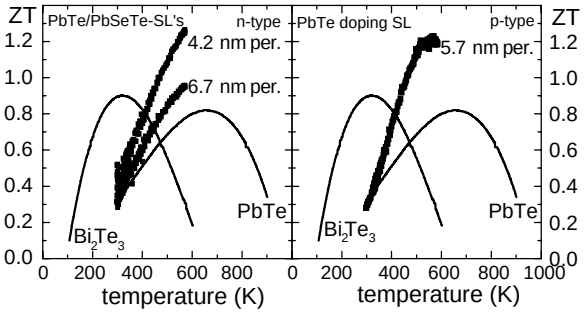

Fig. 3. Determined figures of merit of PbTe-based SL structures compared to bulk IV–VI- and V–VI-alloys [18]. The points denote ZT-values from experimental data of PbTe-based structures (n-type $PbTe/PbSe_{0.2}Te_{0.8}$ SLs with 4.2 nm and 6.7 nm periods (nominal $n = 6 \times 10^{18}$ cm^{-3}, #Pb2, #Pb4)) and a p-type doping SL with 5.7 nm period ($p = 1.2 \times 10^{19}$ cm^{-3}, #Ba2).

several bulk or epitaxial thermoelectric compounds [20] (Bi_2Te_3, PbTe) are compared to the SLs investigated in this study. For Bi_2Te_3-based superlattices, until now, exclusively room temperature measurements were performed.

Temperature-dependent measurements of the thermoelectric properties for PbTe-based superlattices were performed (two $PbTe/PbSe_{0.2}Te_{0.8}$-SLs with 4.2 (#Pb4) and 6.7 nm (#Pb2) period, and one p-type doping SL (#Ba2) with 5.7 nm period). The electrical conductivity was determined by temperature-dependent resistance measurements. These values were used to determine the electronic thermal conductivity λ_{el} by the Wiedemann–Franz law. Beginning from the room temperature values shown before, a decrease of the Lorentz number to 1.6×10^{-8} W Ω K^{-2} for $n = 6 \times 10^{18}$ cm^{-3} (#Pb4: $\lambda_{el,300K} = 0.68$ W m^{-1} K^{-1}; #Pb2: $\lambda_{el,300K} = 0.79$ W m^{-1} K^{-1}) and to 1.75×10^{-8} W Ω K^{-2} for $n = 1.2 \times 10^{19}$ cm^{-3} ($\lambda_{el,300K} = 0.87$ W m^{-1} K^{-1}) at $T = 570$ K was taken into account according to Ref. [17]. The lattice thermal conductivity was estimated from the room temperature λ_{latt}-values (for #Pb2 $\lambda_{latt} = 1.35$ W m^{-1} K^{-1} at $T = 300$ K was estimated from data in Fig. 1) using the T^{-1}-dependence of λ_{latt} for crystalline materials at high temperatures. The maximum values for ZT are ZT = 0.95 for the n-type $PbTe/PbSe_{0.20}Te_{0.80}$-SL with 6.7 nm period and ZT = 1.25 for the SL with 4.2 nm period at $T = 570$ K (nominal $d_{PbSeTe} = 1.8$ nm). For the p-type doping SL with 5.7 nm period (nominal 0.8 nm BaF_2-doped layer), the evaluation results in a figure of merit of ZT = 1.2 at $T = 500$ K.

In conclusion, our results show the suitability of Bi_2Te_3- and PbTe-based superlattice structures for highly efficient thin film thermoelectric applications. In both material systems, ZT-values of homogeneous epitaxial films are surpassed by SL structures at $T = 300$ K. So far, in the Bi_2Te_3-based SLs, the figures of merit are comparable to those of the bulk material; for the PbTe-based SLs, these values are higher than the corresponding ones for bulk PbTe in the temperature range from 300 to 550 K. Around $T = 500$ K, all the thin film thermoelectric materials used so far have worser figures of merit ZT.

This work was supported by the German Ministry for Education and Research (BMBF, Grant No. 03N2014A). Temperature-dependent thermopower and electrical resistance measurements were performed by U. Starke and J. Schumann at IFW Dresden. Fruitful discussions with F. Völklein (FH Wiesbaden) are gratefully acknowledged.

References

[1] T.M. Tritt (Ed.), Recent Trends in Thermoelectric Materials Research III, Academic Press, New York, 2001.
[2] T.C. Harman, et al., J. Electron. Mater. 25 (1996) 1121.
[3] H. Beyer, et al., Proceedings of the 18th International Conference on Thermoelectrics, 1999, p. 416.
[4] R. Venkatasubramanian, in: T.M. Tritt (Ed.), Recent Trends in Thermoelectric Materials Research III, Academic Press, New York, 2001.
[5] A. Balandin, et al., Phys. Rev. B 58 (1998) 1544.
[6] A. Balandin, et al., J. Appl. Phys. 84 (1998) 6149.
[7] T. Yao, Appl. Phys. Lett. 51 (1987) 1798.
[8] S.-M. Lee, et al., Appl. Phys. Lett. 70 (1997) 2957.
[9] R. Venkatasubramanian, et al., Proceedings of the 17th International Conference on Thermoelectrics, 1998, p. 191.
[10] A. Kiselev, et al., Phys. Rev. B 62 (2000) 6896.
[11] X. Fan, Appl. Phys. Lett. 78 (2001) 1580.
[12] T.C. Harman, et al., J. Electron. Mater. 28 (1999) L1.
[13] T.C. Harman, et al., J. Electron. Mater. 29 (2000) L1.
[14] J. Nurnus, et al., Proceedings of the 19th International Conference on Thermoelectrics, 2000, p. 236.
[15] H. Beyer, et al., Proceedings of the 19th International Conference on Thermoelectrics, 2000, p. 28.
[16] F. Völklein, et al., Measurement 5 (1987) 38.
[17] C.M. Bhandari, et al., J. Phys. D 18 (1985) 873.
[18] H.J. Goldsmid, Electronic Refrigeration, Pion Limited, London, 1986, ISBN 0 85086 119 5.
[19] A.F. Ioffe, Dokl. Akad. Nauk SSSR 106 (1956) 981.
[20] G. Min, et al., Appl. Phys. Lett. 77 (2000) 860.